AIAA 81-1283R

Transverse Acoustic Waves in Pulsed Lasers

Charles J. Knight*
Avco Everett Research Laboratory, Inc., Everett, Mass.

Transverse acoustic waves in pulsed lasers result from nonuniform pumping transverse to the flow direction. This theoretical study is based on linear acoustics and disregards hot/cold gas interfaces. First, transverse waves in an infinite parallel hard-walled duct are considered, in which case cavity medium inhomogeneity typically decays as $t^{-1/2}$. An idealized treatment is next given to show that exponential decay can be expected with an anode absorber. There is an optimum absorber resistivity and improved attenuation rate results with increased backing volume. Tilted sidewalls are the final topic. Decay is again exponential, and rapid attenuation requires fairly large tilt angles. Examples are chosen to apply to CO_2 electric discharge, chemical, and excimer lasers.

I. Introduction

ATTENUATION of acoustic waves is a key factor in repetitively pulsed gas laser systems because it determines the minimum intrapulse time and hence the achievable rep-rate. The waves arise from waste heat added to the cavity gas during the laser pumping process. The pulse duration is almost invariably short compared to the acoustic transit time across the cavity, so the result is overpressure within the pumped region. Longitudinal acoustic waves (i.e., in the flow direction) are normally the most evident phenomena in pulsed lasers and can dictate performance. They have been treated in several recent publications based on quasi-one-dimensional transient modeling.[1-6] Waves moving predominantly transverse to the flow direction also arise and have received less attention. They generally require two-dimensional modeling. Transverse waves can be important in advanced pulsed laser systems which require ever-improving acoustics technology.

Typical open- and closed-cycle pulsed laser configurations are depicted in Fig. 1. Only subsonic flow is of concern here. Examples of open-cycle devices are CO_2 electric discharge lasers and HF/DF chemical lasers. In the first case the usual reason for displacing the electrode rods, defining the energy deposition region or cavity, from the sidewalls is to protect the e-beam foil. Electrodes can also be displaced to allow thermal boundary layers to pass outside the laser cavity. In the case of chemical lasers, inert gas layers are used to avoid spontaneous ignition of the laser mixture by walls heated by previous pulses. In either case the displacement of the cavity downstream of the choked flow plate should be kept as small as possible to achieve high rep-rate. Such devices should operate at low flow Mach number to achieve good stored-mass utilization efficiency.

Excimer lasers are closed-cycle devices because the gases involved are too expensive to throw away. In this case the cavity gas is usually pumped by opposed, high current density e-beams and the energy deposition extends all the way to the sidewalls. There are exceptions to this, such as discharge-pumped excimer lasers with electrodes displaced into the flow. However, the situation depicted in Fig. 1 will be adequate for this discussion. Closed-cycle lasers operate at Mach numbers in the 0.2-0.5 range if the objective is to achieve as much average output power as possible from the gas within the flow loop, consistent with reasonable recirculator power.

Presented as Paper 81-1283 at the AIAA 14th Fluid and Plasma Dynamics Conference, Palo Alto, Calif., June 23-25, 1981; submitted July 16, 1981; revision received Nov. 12, 1981.

*Principal Research Scientist. Member AIAA.

In both types of configurations, the energy deposition transverse to the flow direction can be nonuniform within the cavity. For open-cycle devices this is sometimes small compared to the effect of essentially no energy deposition between the cavity and sidewalls and will be overlooked here. An exception is noted in Sec. III. On the other hand, nonuniform energy deposition is the key factor leading to transverse acoustic waves in a typical excimer laser configuration. This normally involves energy deposition which is symmetrical about the centerline of the flow channel and the amplitude of the nonuniformity is relatively small. The effect remains significant because the output laser wavelength is small ($\lambda \lesssim 0.5$ μm), implying a more stringent medium homogeneity requirement.

In a single paper there is little possibility of covering all the transverse wave attenuation processes that can be appropriate for such a broad class of pulsed lasers. Instead a few examples are chosen as illustrative: 1) two-dimensional waves in an infinite, parallel, hard-walled duct with baseline flow; 2) purely transverse waves between parallel walls with an absorber on one wall; and 3) the effect of tilted sidewalls in an idealized configuration.

Fully nonlinear effects tend to require sophisticated computational techniques and are usually restricted to a particular configuration due to cost. This paper concentrates on more generality in configuration, and less in detailed accuracy, by restricting attention to the linear acoustics regime. That is not a bad approximation for excimer lasers, but is restricted to late times for chemical and most electric discharge lasers. Hot/cold gas interfaces will also be avoided to simplify the analysis. Their main effect is to increase the transverse wave clearing time somewhat by reducing radiation

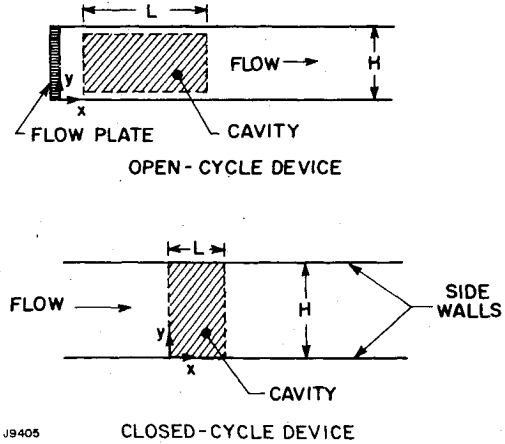

Fig. 1 Typical pulsed laser configurations.

of acoustic energy out of the waste-heated gas zone. This generally is not the prime mechanism for transverse wave decay in a properly designed acoustic attenuator system.

II. Waves Between Hard Parallel Walls

The discussion will begin with the simplest two-dimensional situation. Consider the closed-cycle configuration shown in Fig. 1 and imagine that a constant area flow channel is involved which extends to $x=\pm\infty$. In a real closed-cycle system, of course, there will be a contraction section upstream of the cavity and a diffusor downstream. A means of relating this situation to an open-cycle device will be noted later. The sidewalls are taken to be impermeable and acoustically hard throughout this section.

There will actually be a residual overtemperature zone originating from the cavity at each pulse, but hot/cold gas interfaces are going to be overlooked to simplify the analysis. The linearized two-dimensional acoustic equations with baseline flow are then

$$\frac{\partial p'}{\partial t}+\bar{u}\frac{\partial p'}{\partial x}+\gamma\bar{p}\left(\frac{\partial u'}{\partial x}+\frac{\partial v'}{\partial y}\right)=0$$

$$\bar{\rho}\left(\frac{\partial u'}{\partial t}+\bar{u}\frac{\partial u'}{\partial x}\right)+\frac{\partial p'}{\partial x}=0$$

$$\bar{\rho}\left(\frac{\partial v'}{\partial t}+\bar{u}\frac{\partial v'}{\partial x}\right)+\frac{\partial p'}{\partial y}=0 \tag{1}$$

where overbars denote (constant) baseline flow properties and primes denote perturbations about that state. These equations can be put into nondimensional form by introducing the variables $\tilde{t}=\bar{a}t/L$, $\tilde{x}=x/L$, $\tilde{y}=y/L$, $\tilde{p}=p'/\Delta p_i$, $\tilde{u}=\bar{\rho}\bar{a}u'/\Delta p_i$, and $\tilde{v}=\bar{\rho}\bar{a}u'/\Delta p_i$ where L is the cavity length in the flow direction, $\bar{a}=\sqrt{\gamma\bar{p}/\bar{\rho}}$ is the baseline sound speed, and Δp_i is a mean initial overpressure in the cavity. The baseline Mach number $M=\bar{u}/\bar{a}$ and the aspect ratio $\eta=H/L$ will also enter the analysis.

Cavity medium density homogeneity is a key parameter in a laser system since it can dictate the output beam's optical quality. Here rms tilt and sphere are *not* removed, to simplify evaluation. Also, attention is restricted to times $\tilde{t}>1/M$. This represents no serious constraint in practice because $\tilde{t}>1/M$ is required to clear waste-heated gas from the cavity anyway. Density and pressure distributions then follow an isentropic relationship and therefore a relevant measure of density uniformity is

$$\left(\frac{\delta\rho}{\rho}\right)_{\text{rms}}=\frac{\Delta p_i}{\gamma\bar{p}}\sqrt{\frac{1}{\eta}\int_0^1\int_0^\eta[\tilde{p}(\tilde{x},\tilde{y},\tilde{t})-\tilde{p}_c(\tilde{t})]^2\,d\tilde{x}\,d\tilde{y}} \tag{2}$$

where the mean cavity pressure

$$\tilde{p}_c=\frac{1}{\eta}\int_0^1\int_0^\eta\tilde{p}(\tilde{x},\tilde{y},\tilde{t})\,d\tilde{x}\,d\tilde{y} \tag{3}$$

In the remainder of this section the tildes will be dropped for notational simplicity with the understanding that only nondimensional variables will be used.

A. Transverse Wave Decay

The succeeding analysis is considerably simplified by working in a reference frame moving with the baseline flow. This is accomplished by introducing the Lagrangian coordinate $\xi=x-Mt$ and results in acoustic equations which have the same form as the nondimensional equivalent of Eq. (1) but for $M=0$. The boundary condition $v=0$ on the sidewalls implies that the solution can be written as

$$p=\sum_{n=0}^{\infty}p_n(\xi,t)\cos(n\pi y/\eta)$$

$$u=\sum_{n=0}^{\infty}u_n(\xi,t)\cos(n\pi y/\eta)$$

$$v=\sum_{n=1}^{\infty}v_n(\xi,t)\sin(n\pi y/\eta) \tag{4}$$

The Fourier modes are decoupled and the following equations hold.

$$\frac{\partial p_n}{\partial t}+\frac{\partial u_n}{\partial\xi}+\frac{n\pi}{\eta}v_n=0$$

$$\frac{\partial u_n}{\partial t}+\frac{\partial p_n}{\partial\xi}=0$$

$$\frac{\partial v_n}{\partial t}-\frac{n\pi}{\eta}p_n=0 \tag{5}$$

The appropriate initial conditions for a pulsed laser at $t=0$ are $u_n=v_n=0$ everywhere, $p_n=A_n$ within the cavity $(0<\xi<1)$, and $p_n=0$ elsewhere. Only the single pulse situation will be considered. The Sommerfeld radiation condition must hold for $\xi\to\pm\infty$.

This problem is best solved by means of Laplace transforms. Define

$$\hat{p}_n(\xi,s)=\int_0^\infty p_n(\xi,t)e^{-st}\,dt$$

etc. By transforming Eq. (5), deriving solutions in $\xi<0$, $0<\xi<1$, and $\xi>1$, and requiring $\hat{p}_n$ and $\hat{u}_n$ to be continuous at the interfaces, the following results are obtained:

$$\hat{p}_n=\frac{\eta s}{n\pi}\hat{v}_n=\frac{sA_n}{2\lambda_n^2}(1-e^{-\lambda_n})e^{\lambda_n\xi} \qquad \xi<0$$

$$=\frac{sA_n}{2\lambda_n^2}[2-e^{-\lambda_n\xi}-e^{-\lambda_n(1-\xi)}] \qquad 0<\xi<1$$

$$=\frac{sA_n}{2\lambda_n^2}(e^{\lambda_n}-1)e^{-\lambda_n\xi} \qquad \xi>1 \tag{6}$$

and $s\hat{u}_n=-\partial p_n/\partial\xi$. Here $\lambda_n=\sqrt{s^2+(n\pi/\eta)^2}$ and the branch of the square root is to be chosen such that $Re(\lambda_n)>0$ for $|s|\to\infty$ with $Re(s)>0$.

These Laplace transforms can be inverted analytically but the results are not overly convenient to use. Instead, asymptotic evaluations for late times will be given. Only the case of $M>0$ and $n>0$ is treated. Attention is also restricted to $t>1/M$, as required to clear waste-heated gas, so that the cavity lies wholly in $\xi<0$. Applying the complex inversion formula gives

$$p_n(x,t)=\frac{1}{2\pi i}\int_{\beta-i\infty}^{\beta+i\infty}\frac{sA_n}{2\lambda_n^2}(1-e^{-\lambda_n})e^{\lambda_n x}e^{(s-M\lambda_n)t}\,ds \tag{7}$$

in lab coordinates, with the cavity in $0<x<1$. The integral is to be evaluated for $t\to\infty$ with $x=0(1)$, and the natural approach is the method of steepest descents.[7]

Saddle point locations follow from $d(s-M\lambda_n)/ds=0$, and this leads to $s=\pm i\sigma_n$ with $\sigma_n=n\pi/\eta\sqrt{1-M^2}$. Also,

$$s\sim\pm i\sigma_n+(i\mp1)Mz\sqrt{\sigma_n/(1-M^2)} \tag{8}$$

near the respective saddle points with z real. The curve of steepest descent is thus as depicted in Fig. 2, where the dashed

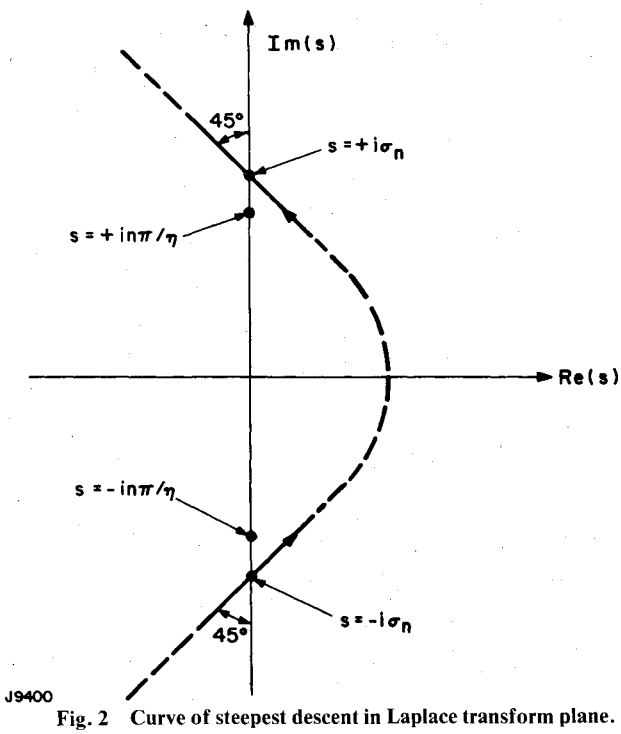

Fig. 2 Curve of steepest descent in Laplace transform plane.

portions are relatively arbitrary since the dominant contributions to the integral in Eq. (7) arise from the immediate vicinity of the saddle points. The arrows on the contour indicate the direction of increasing z. Note that the saddle points lie outside of the branch points of $\hat{p}_n$ since $\sigma_n > n\pi/\eta$ for $0<M<1$. No singularities need be crossed in deforming the integration contour. Application of the method of steepest descents gives

$$p_n \sim -\frac{A_n}{M}\sqrt{\frac{2}{(1-M^2)\pi\sigma_n t}}\sin\left(\frac{M\sigma_n}{2}\right)\sin(\psi) \quad t\to\infty \tag{9}$$

where $\psi = M\sigma_n(x-1/2)+(1-M^2)\sigma_n t-\pi/4$. An independent asymptotic evaluation is possible for $M=0$ by considering only the contributions to $\hat{p}_n$ near its branch points. This agrees with the limiting form of Eq. (9) and serves as a check.

The envelope defining the decay of the transverse wave field between hard parallel walls is $t^{-1/2}$ according to linear theory. Kulkarny[8] has considered the effect of nonlinear wave-overtaking processes on transverse wave decay and has shown that will modify the decay envelope to $t^{-4/5}$. This ramification is not pursued here because there are other loss mechanisms, considered later in the paper, which lead to exponential rather than algebraic decay.

B. Cavity Medium Homogeneity

The next step is to add up contributions from the Fourier components to establish the manner in which cavity medium density homogeneity is restored. Recognize that the mean cavity pressure in Eq. (3) will be zero once the longitudinal rarefaction waves have cleared the cavity $[t>1/(1-M)]$ and that this will have occurred by the time the waste-heated gas zone clears the cavity since $M<0.5$ typically. Thus, for $t>1/M$, substitution of the Fourier representation for p into Eq. (2) leads to

$$\left(\frac{\delta\rho}{\rho}\right)_{\text{rms}} = \frac{\Delta p_i}{\gamma\bar{p}}\sqrt{\frac{1}{2}\sum_{n=1}^{\infty}\int_0^1 p_n^2(x,t)\,dx} \tag{10}$$

Only the transverse wave components contribute to homogeneity at late times in a configuration which does not involve longitudinal wave reflection back into the laser cavity.

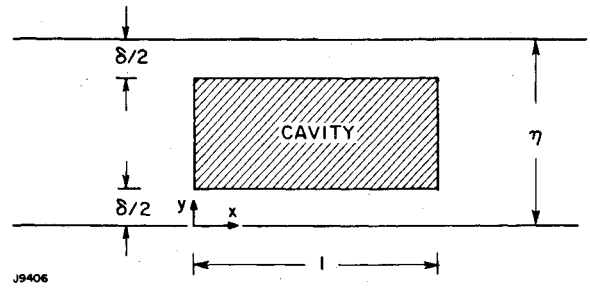

Fig. 3 Displaced energy loading in an infinite duct.

To proceed further it is necessary to define the Fourier coefficients A_n and hence the nature of the energy loading in the laser cavity. Suppose first that the pumped region does not extend all the way to the sidewalls, as depicted in Fig. 3. It will be adequate to consider the case of top-hat energy deposition: $p(x,y,0)=1$ in $0<x<1$ and $\delta/2<y<\eta-\delta/2$ and $p(x,y,0)=0$ otherwise for $t=0$. Then

$$A_n = -\frac{4}{n\pi}\sin\left(\frac{n\pi\delta}{2\eta}\right) \quad n \text{ even}, \quad n>0$$
$$=0 \quad n \text{ odd} \tag{11}$$

This is the situation considered by Kulkarny.[8] He did not, however, explicitly relate his late time pressure field to overall cavity homogeneity.

By now a question should have occurred. The energy loading considered is typical of open-cycle devices but there is no flow plate in Fig. 3. The flow plate is avoided because it complicates the analysis. Consider the following rationale. The upstream edge of the cavity is typically going to be as close to the flow plate as possible to speed longitudinal wave clearing, so going to the extreme of zero displacement is a desirable ideal. It is also true that a flow plate at low Mach number behaves essentially as a hard wall[2] and that a hard wall is mathematically equivalent to a line of symmetry. On this basis the configuration in Fig. 3 can be viewed as somewhat analogous to an open-cycle device. When choosing the aspect ratio η for an open-cycle device, remember that the cavity length in the flow direction is doubled in reflecting about the flow plate.

Only the late time situation will be considered. Substitution of Eq. (9) into Eq. (10) leads to

$$\left(\frac{\delta\rho}{\rho}\right)_{\text{rms}} \sim \frac{\Delta p_i}{\gamma\bar{p}}\sqrt{\sum_{n=1}^{\infty}\frac{\eta F A_n^2\sin(M\sigma_n/2)}{2nt\pi^2M^2\sqrt{1-M^2}}} \quad t\to\infty \tag{12}$$

where $F=1-\sin(M\sigma_n)\sin[(1-M^2)\sigma_n t]/M\sigma_n$. Since F is always upper bounded by $1+\sin(M\sigma_n)/M\sigma_n$, a majorizing series can be introduced which is time-independent. With A_n given in Eq. (11), a short exercise then leads to

$$\left(\frac{\delta\rho}{\rho}\right)_{\text{rms}} \le K\frac{\Delta p_i}{\gamma\bar{p}}(1-M^2)^{-1/4}(\eta t)^{-1/2} \quad t\to\infty \tag{13}$$

where

$$K = \frac{1}{\pi^2\mu}\left\{\sum_{m=1}^{\infty}\left(\frac{1}{m}\right)^3\sin^2\left(\frac{m\pi\delta}{\eta}\right)\sin^2(m\pi\mu)\times\left[1+\frac{\sin(2m\pi\mu)}{2m\pi\mu}\right]\right\}^{1/2} \tag{14}$$

where $m=n/2$ and $\mu = M/\eta\sqrt{1-M^2}$. Medium homogeneity is restored more rapidly in a high aspect ratio cavity (i.e., $\eta \gg 1$),

as expected, but the effect of increasing η is not dramatic.

The coefficient K has been evaluated numerically to arrive at the plots in Fig. 4. The curves are symmetrical about $\delta/\eta = 0.5$ and the maximum value of K always occurs when the cavity displacement from each sidewall, $\delta/2$, is equal to $\eta/4$. It appears that $K \to \infty$ logarithmically as $\mu \to 0$ for any value of δ/η different from 0 or 1. The meaning of this paradoxical result is not clear. It may be that homogeneity is restored somewhat slower than $t^{-1/2}$ for $M=0$. All open-cycle devices in the author's experience involve $\mu < 1$. However, for completeness, it should be noted that $K=0$ for integer values of $\mu \geq 1$. This does not mean medium inhomogeneity due to transverse waves is eliminated. Rather the next term in the asymptotic expansion for p at late time, which is believed to be proportional to $t^{-3/2}$, is dominant at those points.

In the case of e-beam pumped devices, which are typically closed-cycle excimer lasers, the cavity extends all the way to the sidewalls. The source of transverse acoustic waves is then nonuniform energy deposition. Rather than detailing how this nonuniformity arises, the discussion will start by assuming only the second-order transverse wave mode is present. This is normally the dominant contributor when opposed e-beams are involved. Thus, within the cavity,

$$p = 1 + \frac{\Delta Q}{Q} \cos\left(\frac{2\pi y}{\eta}\right) \quad \text{at } t=0 \tag{15}$$

where $\Delta Q/Q$ defines the degree of nonuniformity and is typically less than 20%. The majorized form of Eq. (12) in this case becomes

$$\left(\frac{\delta\rho}{\rho}\right)_{\text{rms}} \lesssim C \frac{\Delta Q}{Q} \frac{\Delta p_i}{\gamma \bar{p}} (1-M^2)^{-3/4} (\eta t)^{-1/2} \quad t \to \infty \tag{16}$$

where

$$C = \frac{\sin(\pi\mu)}{2\pi\mu} \sqrt{1 + \frac{\sin(2\pi\mu)}{2\pi\mu}} \tag{17}$$

and $\mu = M/\eta\sqrt{1-M^2}$ as before. The coefficient C is plotted in Fig. 5. Again, $\mu < 1$ for all lasers in the author's past experience and the zeros of C for integer $\mu \geq 1$ mean nothing more than somewhat faster restoration of homogeneity at those points.

Simple radiation of acoustic energy out of the laser cavity is an obvious explanation for transverse wave decay and has long been accepted. However, it clearly involves slower restoration of cavity medium homogeneity than is acceptable or observed. Other mechanisms must be important, at least for well-designed acoustic attenuator systems. A general understanding of all important processes is not available at this time. However, the examples in the next two sections show that there are mechanisms which can damp transverse waves at a rate much faster than $t^{-1/2}$.

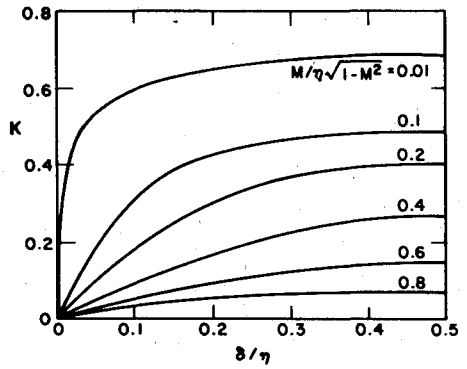

Fig. 4 Homogeneity coefficient for displaced cavity.

III. Attenuation with a Sidewall Absorber

Parallel sidewalls, which are only partially reflecting, generally lead to exponential decay of transverse waves. Finite sidewall acoustic impedance can arise in any of the pulsed lasers mentioned in Sec. I, but it is really most relevant to electric discharge lasers in which a sidewall muffler is intentionally placed behind the anode.[9] The e-beam foil and vacuum chamber is usually placed behind the cathode, so there can be a muffler on only one side. To avoid undue difficulty in the analysis, only the case of purely transverse waves is considered in this section. That is, the waves are taken to move normal to the baseline flow direction so that a one-dimensional problem results. This is an ad hoc idealization, but it is plausible with strong sidewall attenuation because radiation of acoustic energy from the cavity is a relatively slow process based on the previous section.

Energy deposition in a CO_2 electric discharge laser usually involves structure beyond a top-hat profile.[10] There can be a linear gradient between cathode and anode due, in part, to scattering of the e-beam by the gas. There is also a thin cathode-fall region where ions are rapidly accelerated in a narrow zone near the cathode to produce locally enhanced Joule heating and the well-known cathode waves. Both of these are discussed in Ref. 10. Nonetheless, for the purpose of this paper it will be adequate to consider only the case of top-hat deposition between electrodes. The same basic methodology applies generally.

Consider the configuration depicted in Fig. 6. The one-dimensional version of Eq. (1) applies in the flow channel, $0 < y < H$. These equations are not appropriate in the backing volume, $H < y < H+h$, where porous acoustic absorbing material is generally placed. An adequate model for the perturbed continuity and momentum equations in a porous media is provided by[11]

$$\epsilon \frac{\partial \rho'}{\partial t} + \bar{\rho} \frac{\partial v'}{\partial y} = 0 \qquad \frac{k\bar{\rho}}{\epsilon} \frac{\partial v'}{\partial t} + \frac{\partial p'}{\partial y} = -fv' \tag{18}$$

where v' is the speed of volume displacement, ϵ the porosity or void fraction, k the structure factor accounting for path

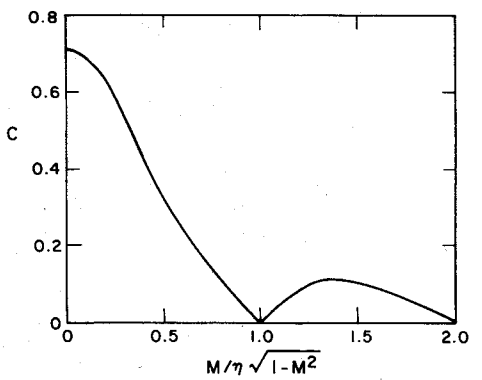

Fig. 5 Homogeneity coefficient for second-order nonuniformity.

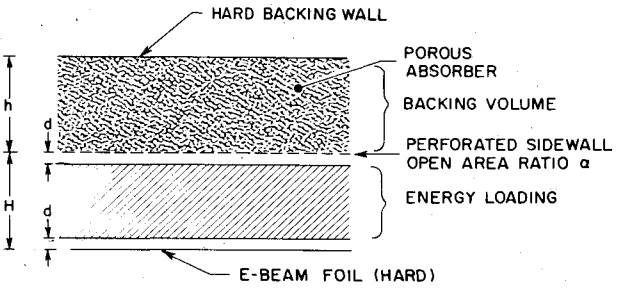

Fig. 6 Idealized anode muffler configuration.

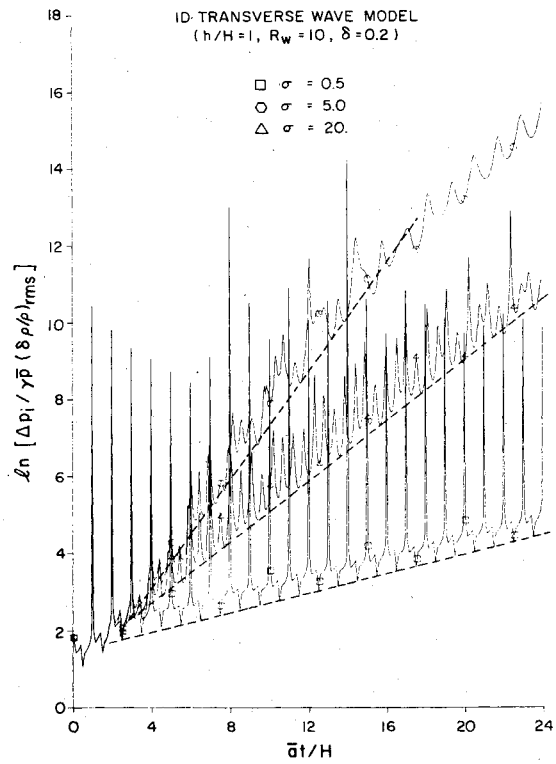

Fig. 7 Restoration of medium homogeneity with an anode muffler.

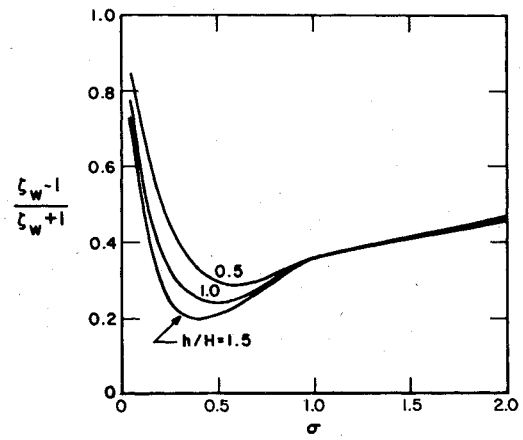

Fig. 8 Effective reflection coefficient of perforated sidewall.

tortuosity, and f the flow resistivity for the acoustic absorber. To be strictly correct, an energy equation should be added to account for heat transfer within the backing volume. However, it will be adequate to assume a polytropic process

$$p'/\bar{p}=n\rho'/\bar{\rho} \tag{19}$$

where $1\le n\le\gamma$, the adiabatic index.

The boundary conditions clearly involve $v'=0$ on $y=H$ and $y=H+h$ since hard walls are assumed there. Due to its definition, v' must also be continuous across the perforated sidewall as long as compressibility effects are unimportant. This does not mean that v' is constant through the perforated plate because the flow must accelerate and decelerate with open-area ratio $\alpha<1$. Rather, it applies outside a jet coalescence distance on each side, with very small coalescence distance. While this treatment is strictly valid only if the diameter of each perforation is infinitesimal, it should provide a reasonable approximation if the diameter is small compared to cavity and backing volume dimensions, as is usually true.

In general the mass exchange process through the perforated sidewall can be expected to be in the nonlinear regime for CO_2 electric discharge lasers. This is true because medium homogeneity requirements can be met with relatively strong waves still in the cavity (e.g., $\gtrsim$ 130 dB). Here constant orifice discharge coefficient C_D will be assumed. Then, for small overpressure, the velocity within each orifice is

$$v_0'=\pm C_D\sqrt{\pm\,(2/\bar{\rho})\,(p_f'-p_b')} \tag{20}$$

where f and b denote evaluation at $y=H-0$ and $y=H+0$, respectively, the upper signs are to be used if $p_f'>p_b'$, and the lower signs are to be used if $p_b'>p_f'$. It is implicitly assumed that there is a gap between the perforated sidewall and the porous absorber in the backing volume. The gap will be taken to have negligible dimension in what follows as is appropriate with small diameter, closely spaced orifices. With grazing flow, Eq. (20) should be okay for $p'\gtrsim 0.3\,\bar{\rho}\bar{u}^2$ where $\bar{u}$ is the baseline flow speed.[12] The velocity within each orifice can be eliminated since $\alpha v_0'=v_f'=v_b'$, where α is the open-area ratio of the perforated sidewall.

The following nondimensional variables will be used: $\tilde{t}=\bar{a}t/H$, $\tilde{y}=y/H$, $\tilde{p}=p'/\Delta p_i$, $\tilde{v}=\bar{\rho}\bar{a}v'/\Delta p_i$, $d=D/H$, and $\tilde{h}=h/H$. The complete problem can then be stated as

$$\frac{\partial\tilde{p}}{\partial\tilde{t}}+\frac{\partial\tilde{v}}{\partial\tilde{y}}=0 \qquad \text{in } 0<\tilde{y}<1$$

$$\frac{\partial\tilde{v}}{\partial\tilde{t}}+\frac{\partial\tilde{p}}{\partial\tilde{y}}=0$$

$$\frac{\partial\tilde{p}}{\partial\tilde{t}}+\beta\zeta\frac{\partial\tilde{v}}{\partial\tilde{y}}=0 \qquad \text{in } 1<\tilde{y}<1+\tilde{h}$$

$$\frac{\partial\tilde{v}}{\partial\tilde{t}}+\frac{\beta}{\zeta}\frac{\partial\tilde{p}}{\partial\tilde{y}}=-\sigma\tilde{v}$$

$$\tilde{p}=\begin{cases}1, & d<\tilde{y}<1-d\\ 0, & \text{otherwise}\end{cases} \qquad \tilde{v}=0 \text{ at } \tilde{t}=0 \tag{21}$$

$$\tilde{v}=0 \text{ on } \tilde{y}=0 \text{ and } \tilde{y}=1+h$$

$$\tilde{v}_f=\tilde{v}_b,\ \tilde{p}_f-\tilde{p}_b=R_w\,|\tilde{v}_f|\,\tilde{v}_f \text{ on } \tilde{y}=1$$

where $\beta=\sqrt{n/k\gamma}$ is a sound speed ratio, $\zeta=\sqrt{kn/\epsilon^2\gamma}$ is an acoustic impedance ratio, $\sigma=\epsilon fH/k\bar{\rho}\bar{a}$ is a normalized resistivity for the acoustic absorber in the backing volume, and $R_w=\Delta p_i/2\gamma\bar{p}\alpha^2C_D^2$ is a resistance factor for the perforated sidewall in the weakly nonlinear mass exchange regime.

An analytical treatment would not be convenient even for linear mass exchange at the perforated sidewall. However, the more correct nonlinear condition used here assures that numerical techniques must be employed. The method of characteristics is used. Only the case of $\beta=\zeta=1$ is considered, and $R_w=10$ is adopted as representative. Typical results for the cavity medium homogeneity as a function of $\tilde{t}$ are given in Fig. 7. This time rms tilt is removed before computing $(\delta\rho/\rho)_{rms}$. Note that the perforated sidewall is a relatively poor damper by itself. This is interpreted to mean that there are transverse wave modes with velocity nodes near the perforated sidewall, essentially nullifying the vena contracta losses there for those Fourier modes. Increasing the resistivity (i.e., σ) of the porous absorber in the backing volume helps, but only to a point as seen from the fact the decay rate for $\sigma=20$ is less than that for $\sigma=5$. Too much resistance prevents full utilization of the backing volume. This should be expected since $\sigma=\infty$ corresponds in essence to a hard wall at $\tilde{y}=1$.

A log-linear plot is used in Fig. 7 to display the essentially exponential restoration of medium homogeneity in the cavity. The dashed curves in Fig. 7 define a qualitatively correct upper bound to the medium homogeneity at any time and provide a convenient means of showing the dependence of the decay rate on σ and $\bar{h}$. The fit will be stated in terms of an effective reflection coefficient for the perforated sidewall:

$$\left(\frac{\delta\rho}{\rho}\right)_{\text{rms}} \lesssim \frac{\Delta p_i}{\gamma\bar{p}}\left(\frac{\zeta_w - 1}{\zeta_w + 1}\right)^{\bar{a}t/2H} \tag{22}$$

where the factor of 2 in the exponent arises from the fact that there is an absorber on only one sidewall and ζ_w is an effective normalized impedance of the perforated sidewall. To derive this form approximately, the anode muffler should be disregarded and a Robin boundary condition, $\bar{p} = \zeta_w \bar{v}$, should be applied at $\bar{y} = 1$ for constant ζ_w.

Plots of the effective reflection coefficient obtained in this way are given in Fig. 8. There is seen to be an optimum resistivity for each value of $\bar{h}$ and the optimum σ decreases as h increases. In all cases considered, $\delta_w \to 1$ only for $h \to \infty$. An implicit approximation in applying Eq. (22) should be noted. The solution to Eq. (21) will always involve reflection from the perforated sidewall as long as $R_w > 0$. The time to couple acoustic energy through the perforated sidewall is overlooked by drawing the dashed curves in Fig. 7 to fit only for larger values of t. Instantaneous decay of transverse waves, as implied by Eq. (22) for $\delta_w = 1$, will not occur in practice. Proper acoustic design can, however, assure the attenuation is very rapid.

IV. Effect of Tilted Sidewalls

Tilted sidewalls have been part of the folklore on pulsed lasers for about a decade. The basic intent is to "walk" the transverse waves out of the cavity by employing sidewalls that are slanted with respect to the centerline of the flow channel. The argument assumes the waves are given an upstream (or downstream, depending on wall slope) component at each interaction with the sidewall. Tilted sidewalls, or a more general channel height variation, can be applied for any of the pulsed lasers discussed in Sec. I. The effectiveness of this approach will be quantified here for the idealized configuration shown in Fig. 9. The centerline in this orientation is located at $\theta = \theta_w/2$. The cavity is taken to be a segment of a circular annulus so that separation of variables will be possible. Also, only the case of no baseline flow is considered so that the acoustic equations involve constant coefficients. The idealization is drastic, but the main results to be obtained are believed to be representative nonetheless.

Equation (1) can readily be rewritten in cylindrical coordinates. Nondimensional variables are also introduced in the same way as in Sec. II, using the cavity length L and the initial mean overpressure Δp_i. The tildes are again dropped for notational simplicity with the understanding that only nondimensional variables are used hereafter. Finally, the boundary condition $v_\theta = 0$ on the hard sidewalls implies that the solution can be written as

$$p = \sum_{n=0}^{\infty} p_n(r,t)\cos\left(\frac{n\pi\theta}{\theta_w}\right)$$

$$v_r = \sum_{n=0}^{\infty} u_n(r,t)\cos\left(\frac{n\pi\theta}{\theta_w}\right)$$

$$v_\theta = \sum_{n=1}^{\infty} v_n(r,t)\sin\left(\frac{n\pi\theta}{\theta_w}\right) \tag{23}$$

Modes that are both symmetric and antisymmetric about the cavity centerline are included in the summations. The modes are decoupled and the following equations hold

$$\frac{\partial p_n}{\partial t} + \frac{\partial u_n}{\partial r} + \frac{1}{r}(u_n + \nu v_n) = 0$$

$$\frac{\partial u_n}{\partial t} + \frac{\partial p_n}{\partial r} = 0$$

$$\frac{\partial v_n}{\partial t} - \frac{\nu}{r}p_n = 0 \tag{24}$$

where $\nu = n\pi/\theta_w$ is introduced for convenience.

These equations can be solved analytically. However, the Laplace-transformation solution involves modified Bessel functions and is nontrivial to invert—even approximately for late times. Results are more easily obtained with a fully numerical treatment. A characteristics procedure is most convenient. The formulation used here involves an implicit scheme with central differencing in both space and time to avoid spurious numerical dissipation. This treatment does involve some phase error due to numerical dispersion with the grid spacing used, which involved a compromise between accuracy and computational economy. Small phase errors are not a prime concern for the purposes of this paper.

Results have only been generated for the case of a particular distributed initial overpressure distribution extending all the way to the sidewall: $p_0 = 1$ and $p_2 = \Delta Q/Q$ in the cavity at

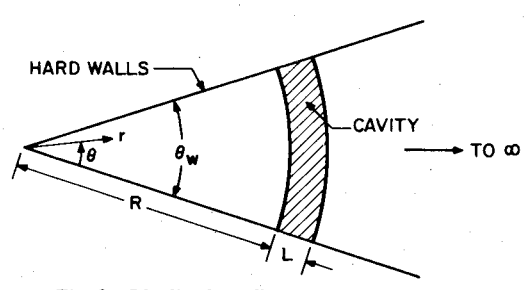

Fig. 9 Idealized configuration with tilted walls.

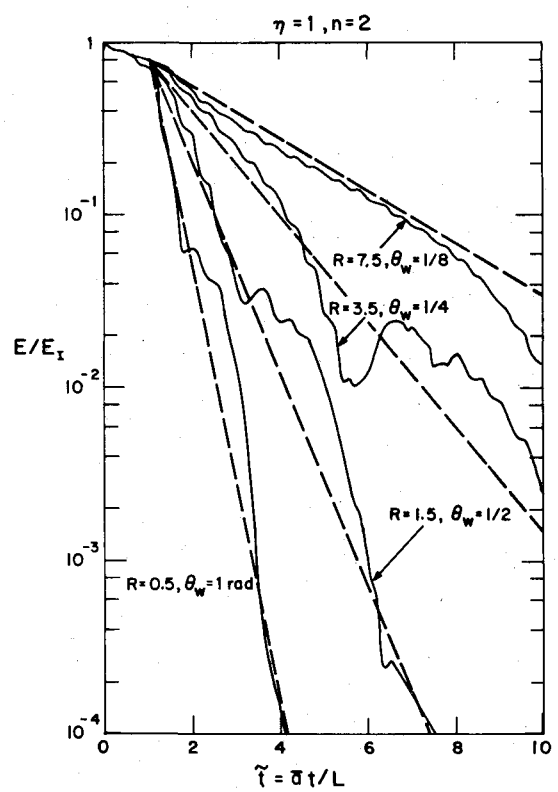

Fig. 10 Transverse acoustic energy decay between tilted walls.

$t=0$, with a top-hat radial distribution. The Cartesian analog is given in Eq. (15). As stated earlier, this situation is most appropriate to e-beam pumped excimer lasers. The values of u_n and v_n are initially zero, variables must be bounded at the origin, and the Sommerfeld radiation condition of outgoing waves only applies for $r\to\infty$.

It will be most useful to display the effect of varying the wall tilt angle θ_w with fixed cavity aspect ratio. This is taken to involve fixed $\eta=(R+\frac{1}{2})\theta_w$ in terms of nondimensional variables. The attenuation of acoustic energy associated with the second-order transverse wave mode displayed as solid curves in Fig. 10 is for $\eta=1$. Here

$$E=\int_R^{R+1}(p_n^2+u_n^2+v_n^2)\,r\,dr \tag{25}$$

and E_i is the value of E corresponding to the initial state

$$E_i=\left(\frac{\Delta Q}{Q}\right)^2(R+\tfrac{1}{2}) \tag{26}$$

for the situation considered. The large bumps in the solid curves for $t\approx 2R$ are due to wave reflection from the vicinity of the origin ($r=0$), as seen in Fig. 9.

The movement of transverse wave energy into the region $r<R$, evidenced by these bumps even for large wall tilt angles, is inconsistent with "walking" transverse waves out of the cavity. All transverse wave energy should be radiated into $r>R$ according to the geometric acoustics viewpoint outlined at the beginning of this section. Nonetheless, weak transmission into $r<R$ occurs by diffraction.

The decay process can be considered to be predominantly exponential, as indicated by the dashed lines in Fig. 10. A useful fit is provided by

$$E\approx 0.8E_i\exp[-2.8\theta_w(t-1)] \qquad t>1 \tag{27}$$

with θ_w in radians. Experimental results for a tilted-wall cavity configuration have been obtained by Morris et al.[13] which give an exponential factor of 3/rad rather than 2.8. In their arrangement there is an area discontinuity in $r>R$, but that would not be expected to be of dominant importance based on geometric acoustics. Details of the configuration can be found in Ref. 13. The cavity aspect ratio was one.

Plots similar to Fig. 10 have been constructed for other aspect ratios. These lead to the conclusion that Eq. (27) applies generally for $1\le\eta\le 2$ provided that θ_w is replaced by θ_w/η. On this basis, the utility of tilted sidewalls is expected to decrease as the cavity aspect ratio increases. Based on the approximate fit, this is due to nothing more than increased transit time between sidewalls as compared to longitudinal wave transit time. The same will be true with the anode absorber discussed in Sec. III.

Decay of transverse wave energy due to radiation only is given by

$$E\sim nE_i/2\eta t \qquad t\to\infty \tag{28}$$

based on Sec. II, with $n=2$ corresponding to Eq. (27). The decay in Fig. 10 for $\theta_w=1/8$ rad is roughly fit by this form for $t\lesssim 4$. Cavity medium homogeneity can be estimated by taking the square root of E/E_i.

V. Conclusion

A theoretical study has been pursued to explore some of the processes affecting transverse acoustic wave attenuation in two prototypical pulsed-laser configurations. Such waves can arise along the optical axis as well as orthogonal to it, so the y direction has not been defined in the paper. However, acoustic waves moving along the optical axis generally have less effect on optical homogeneity. The analysis is based on linear acoustics and disregards hot/cold gas interfaces. For devices involving large initial overpressures (e.g., 1-5 atm), this limits the validity of the results to late times and they are probably only indicative then. The main benefit of making these assumptions is that the analysis becomes relatively straightforward, allowing economical parametric studies. The following conclusions can be drawn from this study.

1) Radiation of transverse acoustic energy out of the laser cavity is a relatively slow process, with medium inhomogeneity scaling as $t^{-\frac{1}{2}}$ based on linear theory. This is typically much slower than is observed experimentally. A quantitative basis is given for estimating restoration of cavity medium homogeneity at late times in a parallel hard-walled duct with baseline flow.

2) Attenuation by a sidewall absorber will produce exponential decay of the transverse wave energy. In the case of an anode muffler, a resistive porous absorber should be placed in the backing volume for good performance. There is an optimum resistivity and improved attenuation rate results with increased backing volume.

3) Tilted sidewalls can also lead to more rapid decay of transverse waves, but the required angles are fairly large for dramatic improvement over simple radiation with parallel sidewalls. When there is baseline flow, this argues that the scheme is best applied with converging walls in the cavity to avoid flow separation. The effect of tilted walls on baseline flow homogeneity must also be examined critically.

Acknowledgments

This work was supported by the Defense Advanced Research Projects Agency of the Department of Defense and was monitored by the U.S. Army Missile Command under Contract DAAK40-78-C-0126.

References

[1] Ausherman, D., Alber, I., and Baum, E., "Acoustic Suppression in a Pulsed Chemical Laser," *AIAA Journal*, Vol. 17, May 1979, pp. 490-497.

[2] Srivastava, B., Knight, C., and Zappa, O., "Acoustic Suppression in a Pulsed Laser," *AIAA Journal*, Vol. 18, May 1980, pp. 555-562.

[3] Thayer, W., Buonadonna, V., and Sherman, W., "Pressure Wave Suppression for a Pulsed Chemical Laser," *AIAA Journal*, Vol. 18, June 1980, pp. 657-664.

[4] Tong, K., Knight, C., and Srivastava, B., "Pressure Wave Attenuation in Mufflers with Finite Backing Volume," AIAA Paper 79-0602, March 1979.

[5] Hogge, D., Crow, S., Morris, J., and Hurdle, P., "Modeling and Simulation of Flow and Acoustics in Pulsed Excimer Lasers," Poseidon Research Rept. No. 21, Santa Monica, Calif., Feb. 1979.

[6] Tong, K., Knight, C., Singh, P., and Srivastava, B., "Flow and Acoustics Study for Pulsed Visible Lasers," AIAA Paper 80-0348, Jan. 1980.

[7] Carrier, G., Krook, M., and Pearson, C., *Functions of a Complex Variable*, McGraw-Hill Book Co., Inc., New York, 1966, Chap. 6.

[8] Kulkarny, V., "Decay of Transverse Acoustic Waves in a Pulsed Gas Laser," *AIAA Journal*, Vol. 18, Nov. 1980, pp. 1336-1341.

[9] Srivastava, B. and Knight, C., "Pressure Wave Attenuation due to Anode Mufflers in Pulsed Lasers," AIAA Paper 81-1282, June 1981.

[10] Pugh, E., Wallace, J., Jacob, J., Northam, D., and Daugherty, J., "Optical Quality of Pulsed Electron-Beam Sustained Lasers," *Applied Optics*, Vol. 13, Nov. 1974, pp. 2512-2517.

[11] Zwikker, C. and Kosten, C., *Sound Absorbing Materials*, Elsevier, New York, 1949, Chap. 2.

[12] Hersh, A., Walker, B., and Bucka, M., "Effect of Grazing Flow on the Acoustic Impedance of Helmholtz Resonators Consisting of Single and Clustered Orifices," AIAA Paper 78-1124, July 1977; also, NASA CR-3177, 1979.

[13] Morris, J., Levin, J., Crow, S., and Hurdle, P., "Further Investigations of Flow and Acoustics in Pulsed Excimer Laser," Poseidon Research Rept. No. 32, Santa Monica, Calif., Aug. 1980.